Atmos. Meas. Tech. Discuss., 8, 3697–3728, 2015
www.atmos-meas-tech-discuss.net/8/3697/2015/
doi:10.5194/amtd-8-3697-2015

Atmospheric Measurement Techniques Discussions

Open Access

Relative drifts and biases between six ozone limb satellite measurements from the last decade

N. Rahpoe[1], M. Weber[1], A. V. Rozanov[1], K. Weigel[1], H. Bovensmann[1], J. P. Burrows[1], A. Laeng[2], G. Stiller[2], T. von Clarmann[2], E. Kyrölä[3], V. F. Sofieva[3], J. Tamminen[3], K. Walker[4], D. Degenstein[5], A. E. Bourassa[5], R. Hargreaves[6,8], P. Bernath[6], J. Urban[7], and D. P. Murtagh[7]

[1]Institute of Environmental Physics, University of Bremen, Otto-Hahn-Allee 1, 28359 Bremen, Germany
[2]Karlsruhe Institute of Technology, Institute for Meteorology and Climate Research, Karlsruhe, Germany
[3]Finnish Meteorological Institute, Helsinki, Finnland
[4]Department of Physics, University of Toronto, Toronto, Canada
[5]Institute for Space and Atmospheric Studies, University of Saskatchewan, Saskatoon, Saskatchewan, Canada
[6]Department of Chemistry, University of York, York, UK
[7]Chalmers University of Technology, Department of Earth and Space Sciences, 41296 Gothenburg, Sweden

[8]Department of Chemistry & Biochemistry, Old Dominion University, Norfolk, VA, USA

Received: 16 February 2015 – Accepted: 17 March 2015 – Published: 10 April 2015

Correspondence to: N. Rahpoe (nabiz@iup.physik.uni-bremen.de)

Published by Copernicus Publications on behalf of the European Geosciences Union.

Abstract

As part of ESA's climate change initiative high vertical resolution ozone profiles from three instruments all aboard ESA's Envisat (GOMOS, MIPAS, SCIAMACHY) in combination with ESA's third party missions (OSIRIS, SMR, ACE-FTS) are to be combined in order to create an essential climate variable data record for the last decade. A prerequisite before combining data is the examination of differences and drifts between the datasets. In this paper, we present a detailed analysis of ozone profile differences based on pairwise collocated measuerements, including the evolution of the differences with time. Such a diagnosis is helpful to identify strengths and weaknesses of each data set that may vary in time and introduce uncertainties in long-term trend estimates.

Main results of this paper indicate that the 6 instruments perform well in the stratosphere particularly between 20 and 40 km with a mean relative difference of ±5 % (middle latitudes) to ±10 % (tropics). Larger differences and variability in the differences are found in the upper troposphere lower stratosphere region and in the mesosphere. The analysis reveals that the relative drift between the sensors is not statistically significant for most pairs of instruments.

1 Introduction

Ozone as the main absorber in the UV wavelength region is one of the crucial atmospheric trace gases which has been investigated extensively in the past 40 years due to its role as a protecting shield against UV radiation that is harmful for living species. Different observation techniques have been used to extract the ozone signal from the troposphere to the mesosphere (Hassler et al., 2014, and references therein).

Due to a limited lifetime of a single space instrument, long-term studies on ozone require a combination of measurements from different instruments to be merged to obtain a coherent climate data record. For this purpose the merging of the datasets from several instruments is one possible method. In order to have the best observations in-

AMTD
8, 3697–3728, 2015

cluded in the merged data, information about biases and drifts is needed for the optimal use of the data. Similar activities on merging are performed by GOZCARDS (Global OZone Chemistry And Related trace gas Data records for the Stratosphere) for SAGE I, SAGE II, ACE-FTS, and MLS-Aura (Froidevaux et al., 2013) and for combination of SAGE II and GOMOS (Kyrölä et al., 2013) and SAGE II and OSIRIS (Bourassa et al., 2014). This paper deals with the intercomparison of six limb ozone data sets in the framework of the ESA (European Space Agency) climate change initiative (O3 CCI).

Each instrument of the CCI datasets have been validated by comparison with correlative measurements to establish the uncertainty and precision (Steck et al., 2007; Dupuy et al., 2009; Mieruch et al., 2012; Tegtmeier et al., 2013; Adams et al., 2014; Eckert et al., 2014; Laeng et al., 2014). One important aspect of this work is that the intercomparisons are carried out for each possible sensor pair. A linear regression model has been applied in order to determine the differences and drifts between all pairs of instruments.

The paper is divided into six sections. In Sect. 2 we describe briefly the instruments and their performance. In Sect. 3 basic formulae and definitions for the pairwise comparisons are summarised. In Sect. 4, an overview of the results from the intercomparisons is provided. In Sect. 5 results are discussed and compared with other similar intercomparisons. A summary of the main results and concluding remarks are given in Sect. 6.

2 Instruments

The six instruments used for the comparison in this work are carried by three different satellites. Three atmospheric chemistry experiments (GOMOS, MIPAS, and SCIAMACHY) are on board the Envisat satellite operated from 2002 to 2012. It flew in a sun-synchronous orbit at altitude of 780 km leading to an orbital period of ≈ 100 min and 14 orbits per day. The ascending node (equator crossing) is 22:00 LT. OSIRIS and SMR aboard Odin are two instruments taking measurements since 2001 and are still op-

AMTD
8, 3697–3728, 2015

erating. ACE-FTS provides measurements since 2004 on SCISAT. All instruments are briefly described in the following subsections. More details on the instruments and their performance can be found in Hassler et al. (2014) and Sofieva et al. (2013).

2.1 GOMOS on Envisat

GOMOS (Global Ozone Monitoring by Occultation of Stars) is the stellar occulation instrument on board the Envisat satellite that exploits the absorption and scattering of stellar light in ultraviolet (UV), visible and near-infra-red wavelengths to retrieve vertical profiles of ozone, NO_2, NO_3, O_2, H_2O, and aerosol extinction (Kyrölä et al., 2004; Bertaux et al., 2010). Ozone number density profiles are retrieved from measurements by the UV-Vis spectrometer in the altitude range ≈ 10–100 km (Kyrölä et al., 2010). The vertical resolution of GOMOS ozone profiles is 2 below 30 and 3 above 40 km with the linear transition between. The estimated uncertainty of the retrieved ozone profiles is 0.5–5 % (Tamminen et al., 2010). In this paper GOMOS ozone profiles processed with IPF 6.0 are used. The outliers and invalid data have been removed by using the data recommendations.

2.2 MIPAS on Envisat

MIPAS (Michelson Interferometer for Passive Atmospheric Souding) aboard Envisat is a middle infrared Fourier transform spectrometer measuring atmospheric emission spectra in limb mode (Fischer et al., 2008). MIPAS measurements include CH_4, H_2O, HNO_3, N_2O, NO_2, HNO_3, HNO_4, N_2O_5, PAN, CH_4, C_2H_2, C_2H_6, CO, H_2CO, HCN, HCOOH, ClO, $ClONO_2$, HOCl CFC-11, CFC-12, HCFC-22, SO_2 and others NO, HNO_3, HNO_4, N_2O_5, PAN, C_2H_2, C_2H_6, CO, HCN, HCOOH, ClO, $ClONO_2$, HOCl, CFC-11, CFC-12, HCFC-22, SO_2, O_3, temperature, and pressure profiles. The high resolution measurements (0.025 cm^{-1}) are performed from 685 to 2410 cm^{-1} (14.6 to 4.15 µm) for the years 2002–2004. The vertical resolution ranges from 3 to 8 km in the altitude range from 6 to 68 km. After an anomaly in the interferometric drive, the operational mode has

AMTD
8, 3697–3728, 2015

been switched to lower spectral resolution with a finer vertical grid (Cortesi et al., 2007). In this work we use the data from 2005 onwards, which is the low-resolution mode that are currently available from MIPAS-IMK version R 220 (Laeng et al., 2014).

2.3 SCIAMACHY on Envisat

SCIAMACHY measures the Earth's atmosphere in three observation modes, i.e. nadir, limb and occultation (Bovensmann et al., 1999, 2002). In limb mode, SCIAMACHY scans the atmosphere in 3.3 km steps vertically and 960 km across-track. The vertical resolution is about 3–4 km. SCIAMACHY covers the wavelengths between 212 and 2386 nm divided into 8 channels. Atmospheric trace gases such as BrO, CH_4, CO, CO_2, H_2O, IO, NO_2, OClO, O_2, O_3, NO_2, SO_2, and aerosol extinction can be retrieved with SCIAMACHY (Bovensmann et al., 2011).

The retrieved SCIAMACHY ozone profiles from the version V2.5 are used in this study (Rozanov et al., 2001) Algorithm, validation, and error analysis are described in Sonkaew et al. (2009); Mieruch et al. (2012), and Rahpoe et al. (2013), respectively.

2.4 OSIRIS on Odin

OSIRIS (Optical Spectrograph and InfraRed Imager System) is the instrument onboard the Odin satellite that was launched on 20 February 2001 (Murtagh et al., 2002; Llewellyn et al., 2004). Odin circles the Earth in a polar, sun-synchronous, near-terminator orbit with an inclination of 97.8° and an ascending node at 18:00 LST (Local Solar Time). OSIRIS measures the ozone number density profiles with a vertical resolution of 1–3 km in a limb mode from 10 to 70 km. The measurement is performed in the optical spectral range of 280–800 nm with a resolution of 1 nm. In this work the OSIRIS ozone data V5.01 have been used (Adams et al., 2014).

AMTD
8, 3697–3728, 2015

Relative drifts and biases between six ozone limb satellite measurements

N. Rahpoe et al.

2.5 SMR on Odin

The second instrument on the Odin satellite is SMR (Submilimeter and Milimeter Radiometer) which uses heterodyne radiometers to measure thermal emission in the frequency range of 486–581 GHz. Atmospheric species measured in the frequency bands at 501.8 and 544.6 GHz are ClO, HNO_3, N_2O, and O_3 (Urban et al., 2005). The vertical resolution of the ozone data is on the order of 2.5–3.5 below 40 km. For this study we use the SMR ozone data version 2.1 processed at the Chalmers University of Technology, Gothenburg, Sweden. The Optimal Estimation Method (OEM) scheme is used to retrieve the ozone VMR from the O_3 line at 501.8 GHz.

2.6 ACE-FTS on SCISAT

The solar occultation instrument ACE-FTS (Atmospheric Chemistry Experiment – Fourier Transform Spectrometer) onboard the Canadian satellite mission SCISAT was launched on 12 August 2003 (Bernath et al., 1999). It measures high-resolution (0.02 cm^{-1}) spectra between 750 and 4400 cm^{-1} (2.2–13 µm). The vertical resolution of the profiles is 3–4 km with a sampling of 1.5–6 km. More than 30 trace gases, temperature, and pressure are retrieved by ACE-FTS using a modified global fit approach based on the Levenberg–Marquardt nonlinear least-squares method (Boone et al., 2005). In this study we use the ACE-FTS ozone profiles version 3.0 retrieved at the University of Waterloo (Boone et al., 2013).

3 Methodology and definitions

In our analyses, we use collocated measurements for each pair of instruments. The collocation criteria chosen depend on the sampling and coverage of the satellite pair. For comparisons with dense samplers (SCIAMACHY and MIPAS), we selected measurements separated by less than 500 km in space and by less than 5 h in time.

AMTD
8, 3697–3728, 2015

In comparisons with ACE-FTS, which has a very low sampling, the time and spatial coincidence criteria selected are 24 h and 1000 km, respectively. For all other pairs, 1000 km and 12 h have been used as a collocation critera. In Table 1 the total number of collocations is listed for all pairs.

The relative difference (δ) and mean relative difference (Δ) of pairwise collocated ozone amount at altitude z are calculated as:

$$\delta_i(z) = 2 \cdot \frac{x_c - x_r}{X_c + X_r}, \qquad \Delta(z) = \sum_i \frac{\delta_i(z)}{N(z)}, \tag{1}$$

where x_c and x_r correspond to the collocated ozone profiles of the comparison instrument (c) and the "reference" instrument (r), respectively, X_c and X_r are average profiles, and $N(z)$ is the number of available pairs at altitude z. The SD of Δ is calculated as follows:

$$\sigma(z) = \sqrt{\frac{\sum_{i=1}^{N(z)} [\delta_i(z) - \Delta(z)]^2}{N(z) - 1}}. \tag{2}$$

In addition to the relative difference we also applied a linear regression to the montly mean relative difference time series for each altitude. The mean relative difference between two instruments is not necessarily a constant but can vary with time. We analyze this time dependence by using a multi-linear regression model:

$$\Delta(t,z) = \alpha(z) \cdot (t - t^*) + \beta(z) + \sum_i^2 [\kappa_i(z) \sin(\omega_i t) + \nu_i(z) \cos(\omega_i t)], \tag{3}$$

where $\Delta(t,z)$ the monthly mean relative difference timeseries for each altitude. The slope $\alpha(z)$ is the "pairwise relative drift" and $\beta(z)$ is the "pairwise relative bias" derived from the regression function.

AMTD
8, 3697–3728, 2015

The term "bias" is avoided here, since the comparison is not based on one reference sensor but rather each sensor is used as a reference. Instead of "bias" the term "pairwise relative bias" and "pairwise relative drift" between two instruments is more appropriate here and refer hereafter to "relative bias" and "relative drift" denoted by the greek symbols $\beta(z)$ and $\alpha(z)$ respectively.

The corresponding uncertainties σ_α and σ_β are calculated from the regression model for each pair of instruments. For the periodic variation periods of 6 and 12 months have been considered with corresponding harmonic functions and parameters $\kappa(z)$, $\nu(z)$. No proxies of the quasi-biennial oscillation or other natural variability has been considered, because natural effects are assumed to cancel out when the differences are calculated. Since MIPAS RR (Reduced Resolution) profiles are only available from January 2005 onwards, February 2005 was used as reference time t^*.

4 Intercomparison results

In this section, we present the pairwise examples of timeseries and global profiles with SCIAMACHY as the reference sensor (this is the only data set under investigation from a dense sampler covering the full Envisat observation period). In Sect. 5 the results from all combinations are discussed. Details from all possible pair combinations can be viewed as contour plots for $\beta(z)$ and $\alpha(z)$ as Supplement.

4.1 Relative difference timeseries

The monthly mean relative difference timeseries of all CCI limb data with respect to SCIAMACHY for different latitude bands are presented in Figs. 1–3.

In the Arctic (70–60° N, Fig. 1) most of the datasets agree to within ±10 % for all altitudes between 25 and 40 km. Best agreement between all datasets is found at 25 km. Above 30 km MIPAS show some pronounced seasonal cycle in the difference. SCIAMACHY tends to be lower above 30 km, ACE-FTS and MIPAS higher than the other

AMTD
8, 3697–3728, 2015

Relative drifts and biases between six ozone limb satellite measurements

N. Rahpoe et al.

data (all within 10 %). GOMOS, SMR, and OSIRIS are in quite close agreement for all altitudes.

At northern mid-latitudes (50–40° N, Fig. 2) the best agreement between datasets is at 30 km and below. At 30 km and above MIPAS and ACE-FTS are somewhat higher than the other datasets; at 40 km SCIAMACHY is in agreement with MIPAS, but not higher than the other datasets by about 10 %.

In the tropics (0–10° N, 3), the best agreement between all datasets is again at 25 km (±5 %), although SMR seems to be noisy here. At 30 km agreement is similar, except that SCIAMACHY shows a consistent positive bias of about +10 %. At 35 km SMR shows a negative bias of about −5 to 10 % and is quite noisy. At 40 km and similar to the mid-latitudes (Fig. 2) MIPAS and SCIAMACHY are in very good agreement but are about 10 % higher on avarage than all other data.

From all these figures it is also evident that the difference timeseries are smoothest for a pair of high dense sampler like MIPAS and SCIAMACHY. Part of the variability seen in the difference time series, thus, are a consequence of the different sampling statistics.

4.2 Global relative drift α and relative bias β from regression model

The two regression parameters: β (relative bias) and α (relative drift) for all satellite instruments with SCIAMACHY as the reference sensor are shown in Fig. 4 for the latitude band 60° S–60° N.

The relative bias β is within ±10 % between 20 and 40 km. An exception is SMR with β peaking up to +25 % at 20 km. Between 40 and 47 km the deviation increases, with exception of MIPAS, all comparison instruments show negative relative bias β with respect to SCIAMACHY as observed before in the timeseries plots. Most probably, this is due to diurnal ozone variations (The collocations with MIPAS are close in local time). Significance (indicated by open cirlces) of β values is different for each comparison instrument relative to SCIAMACHY. Generally β is statistically significant for most of the comparison sensors with exception of MIPAS.

AMTD
8, 3697–3728, 2015

The relative drift α profile is quite similar for all comparison instruments. There is a low drift on the order of $\pm 5\,\%\,\text{decade}^{-1}$ between 25 and 50 km. Above 50 km the relative drift is getting positive up to $15\,\%\,\text{decade}^{-1}$ and below 20 km the drift is very variable. An oscillating pattern between 30 and 45 km in the drift is observed for MIPAS peaking up to $+10\,\%\,\text{decade}^{-1}$. Nevertheless, the drift is not statistically significant for most part of the atmosphere (see the next section for details). Differences between GOMOS and OSIRIS are very small between 20 and 50 km. This indicates a very good overall agreement between GOMOS and OSIRIS, which was reported also earlier by Adams et al. (2014).

5 Discussion

In order to get an overall picture of the pairwise comparisons with each instrument as reference sensor, the vertical distribution of α and β are drawn in Fig. 5 for 30° N–30° S at altitudes between 15 and 50 in 5 km steps. Each colour identifies the reference sensor. The position of the different symbols mark the value of each comparison sensor relative to the reference sensor. This compact representation gives a detailed view of the performance of each sensor.

In the upper troposphere lower stratosphere (UTLS) the β range is large for most of the instruments. At 20 km the β range is still large, except for ACE-FTS which shows smaller β range relative to other instruments. Smallest β range for most of the reference sensors is observed at 25 km which is to within ±5 %. Only, MIPAS and SMR have a slightly larger absolute β with respect to each other. Between 30 and 50 km the β range increases for each sensor and shows different behaviour. Four different groups can be identified between 25 and 50 km. The classification between groups is mainly determined by the vertical β range behaviour. If all comparison sensors show positive relative bias toward the reference sensor, then we classify the reference sensor as "negative relative bias (β) range". Between 25 and 45 km for the latitude band of 30° N–30° S (Fig. 5a), Group I consists of OSIRIS and GOMOS (balanced β range), Group

AMTD
8, 3697–3728, 2015

II includes ACE-FTS (low positive β range), Group III are MIPAS and SCIAMACHY (positive β range), and Group IV is SMR (systematic negative β range).

Balanced β range means that differences to that instrument may be positve or negative without favoring any sign.

ACE-FTS (Group II) shows positive relative bias between 25 and 50 km. Particulary, above 40 km the bias can reach around 10 %. Such a positive bias was reported in an earlier version of ACE-FTS (Dupuy et al., 2009).

In Group III (MIPAS, SCIAMACHY) the β is mainly positive in the stratosphere with respect to the other sensors. Above 40 km SCIAMACHY shows the largest β value with respect to SMR of up to 20 % at 45 km.

Group IV consists of SMR only with negative β values. Below 45 km it is in closer agreement with Group I but gets statistically significantly negative for all altitudes above 45 km.

From this plot we can conclude, that in the altitude range of 45–50 and 15–20 km most of the groups show similar behaviour in sign and β range (SMR is an exception) in the tropics. Between 25 and 45 km, sign and range of β depends on the reference sensor with four distinct groups as discussed before. The derived errors σ_β from the regression analysis for all pairs are shown in Fig. 5b. The errors are between 0.5 and 8 % in the altitude range of 25–50 km. Comparing σ_β with β, one can conclude how significant the "pairwise relative biases" are. Highly statistically significant values ($\beta > 3\sigma_\beta$) can be found for pairs where SMR is involved. Statistically significant β values can be seen for the following pairs: between OSIRIS and MIPAS at 40 km, between MIPAS and SCIAMACHY, and between GOMOS and SCIAMACHY at 30 km, respectively.

At northern middle latitudes (60–30° N), ACE-FTS shows statistically significant β values (Fig. 6a) at 25 and 30 km in comparison with SCIAMACHY.

In the southern middle latitudes (30–60° S) the relative bias range resembles the behaviour of the tropical band.

There is no clear group behaviour for relative drift α in the tropics 30° N–30° S (see Fig. 8). At 25 km the relative drift between OSIRIS and SMR is up to ±28 % decade^{-1}

AMTD
8, 3697–3728, 2015

with σ_α in the order of 6 % decade^{-1}, which indicates a statistically significant relative drift. Hereafter, we consider a drift estimate α to be statistically significant, if it is outside the $\pm 2\sigma_\alpha$ uncertainty interval. At 40 km the drift between MIPAS and SMR is ±20 % decade^{-1}. At 45 km SMR shows a statistically significant drift as a reference sensor with three instruments, e.g., MIPAS (−25 % decade^{-1}), SCIAMACHY (−9 % decade^{-1}), and OSIRIS (−14 % decade^{-1}). From 50 km upwards the range of drifts is increasing for all reference sensors and with GOMOS, SMR, and MIPAS showing the largest range. Diurnal variation may play a significant role here.

In Fig. 9 the range of drifts (α) is shown with corresponding errors for the northern middle latitudes (60–30° N). At 20 km the instruments (OSIRIS/SMR), (GOMOS/SMR), and (GOMOS/MIPAS) show drifts larger than ±10 % decade^{-1} relative to each other. Between 25 and 50 km the relative drifts between MIPAS and SCIAMACHY are statistically significant in the range of 10 to 25 % decade^{-1} (with the exception at 35 km). At 50 km the pairs MIPAS and ACE, SMR and ACE, and OSIRIS and SMR are showing statistically significant drifts relative to each other.

In southern mid-latitudes (30–60° S) at 20 km although the drift values can be as high as 15 % decade^{-1}, but they are not statistically significant (Fig. 10). At 40 km the relative drift between MIPAS and SMR is larger than 10 % decade^{-1} and statistically significant. At 45 km the drift between the sensors with values larger than 10 % decade^{-1} in absolute values is statistically significant.

The drift analysis reveals; that for most of the pairs and altitudes the relative differences are stable with time. The exception is SMR that shows higher relative drifts with respect to 3 out of 5 instruments at 45 km in different latitude bands.

5.1 Comparison to other validation results

Our results can be compared with other validation works as discussed in the following.

Eckert et al. (2014) performed a detailed drift analysis of MIPAS V5 220 to derive a drift corrected trend for the MIPAS ozone time series. We give a glance overview of

AMTD
8, 3697–3728, 2015

their results of drifts between MIPAS and OSIRIS and between MIPAS and ACE-FTS. For the drifts between MIPAS and OSIRIS, they found mostly negative statistically insignificant drifts in the upper stratosphere, with negative statistically significant values in the northern middle latitudes. The drift signs are in agreement with ours if we compare the MIPAS-OSIRIS drifts in the Southern Hemisphere (as light blue squares in Fig. 10). They find statistically insignificant positive drift values in the latitue bin of 30–40° S between 40 and 48 km. We observe a positive drift at 40 and at 45 km respectively that agrees qualitatively with their results. The drifts are in the order of 8–10 % decade^{-1} going down to 2 % decade^{-1} for lower altitudes, in agreement with their findings. In the northern middle latitudes the drifts are in agreement with our results of mainly negative drifts. Even the change of the sign of the drift at 45 km in their work for the latitude bin of 50–40° N is well reproduced in the analysis in this paper (see Fig. 9).

For comparison between MIPAS and ACE-FTS, the sign of the drifts are consistent with our results for the southern middle latitudes. For the northern middle latitude 60–30° N the vertical oscillation behaviour of the drift values are well reproduced and can be consistently compared with our findings.

Adams et al. (2014) made an analysis of differences between OSIRIS V5.07 and GOMOS V6 ozone profiles. In their comparison, mean relative difference values for the tropical band are lower than 5 % for OSIRIS and GOMOS between 20 and 40 km and a bump of −10 % is observed at 40 km in the tropics. In our case, the comparison between OSIRIS 5.01 and GOMOS V6 shows similar mean relative difference value and shape, especially the sign and values of the mean relative difference between 20 and 40 km and the bump at around 40 km in the tropics is observed. The update of the ozone data led to the reduction of the mean relative difference (compared to GOMOS V5) between the two instruments in this specific region. Additionally our investigation confirms the good agreements (β and α range) of GOMOS and OSIRIS as reference sensors.

AMTD
8, 3697–3728, 2015

6 Conclusions

Comparisons of ozone limb/occulation profiles between 6 independent instruments from three platforms have been performed, i.e., Envisat, Odin, and SCISAT. The pair-wise comparison using collocated data have been used to establish the mean relative differences between 15 pairs of instruments. Monthly mean relative difference time series have been used for drift and relative bias β analysis by applying a linear regression model. The two regression parameters of the linear model, the slope α (relative drift) and the intercept β (relative bias) for the reference time of February 2005 have been calculated for different altitudes and latitude bands. Between 20 and 40 km the β is within ±5 % (middle latitudes) to ±10 % (tropics). Large variability in the UTLS region and below this altitude is observed for all pairs. This can be explained by retrieval problems for sensors due to low signal to noise ratios, larger natural variability, and the impact of clouds and aerosols.

Overall the β can be sorted in different groups:

- group I: GOMOS and OSIRIS (balanced β range)
- group II: ACE-FTS (balanced positive β range)
- group III: SCIAMACHY and MIPAS (positive β range)
- group IV: SMR (systematical negative β range)

The relative drifts between the various instruments can be quite large at some altitudes, but because of the short data record (about 10 years), they are mostly statistically insignificant, except for SMR. Statistically significant relative drift is observed for SMR with respect to 3 out of 5 instruments in the upper stratosphere.

The Supplement related to this article is available online at doi:10.5194/amtd-8-3697-2015-supplement.

AMTD
8, 3697–3728, 2015

Acknowledgements. This work has been funded within the frame work of the ESA project OZONE CCI (Climate Change Initiative). We would like to thank the SCIAMACHY IUP-Bremen, MIPAS-IMK, GOMOS-FMI, OSIRIS, SMR, and ACE-FTS groups for providing the data and support for this work. The ACE mission is supported primarily by the Canadian Space Agency.

References

Adams, C., Bourassa, A. E., Sofieva, V., Froidevaux, L., McLinden, C. A., Hubert, D., Lambert, J. -C., Sioris, C. E., and Degenstein, D. A.: Assessment of Odin-OSIRIS ozone measurements from 2001 to the present using MLS, GOMOS, and ozone sondes, Atmos. Meas. Tech. Discuss., 6, 3819–3857, doi:10.5194/amtd-6-3819-2013, 2013. 3700, 3702, 3707, 3710

Bernath, P. F., McElroy, C. T., Abrams, M. C., Boone, C. D., Butler, M., Camy-Peyret, C., Carleer, M., Clerbaux, C., Coheur, P.-F., Colin, R., DeCola, P., De Mazière, M., Drummond, J. R., Dufour, D., Evans, W. F. J., Fast, H., Fussen, D., Gilbert, K., Jennings, D. E., Llewellyn, E. J., Lowe, R. P., Mahieu, E., McConnell, J. C., McHugh, M., McLeod, S. D., Michaud, R., Midwinter, C., Nassar, R., Nichitiu, F., Nowlan, C., Rinsland, C. P., Rochon, Y. J., Rowlands, N., Semeniuk, K., Simon, P., Skelton, R., Sloan, J. J., Soucy, M.-A., Strong, K., Tremblay, P. Turnbull, D., Walker, K. A., Walkty, I., Wardle, D. A., Wehrle, V., Zander, R., and Zou, J.: Atmospheric Chemistry Experiment (ACE): mission overview, Geophys. Res. Lett., 32, L15S01, doi:10.1029/2005GL022386, 2005. 3703

Bertaux, J. L., Kyrölä, E., Fussen, D., Hauchecorne, A., Dalaudier, F., Sofieva, V., Tamminen, J., Vanhellemont, F., Fanton d'Andon, O., Barrot, G., Mangin, A., Blanot, L., Lebrun, J. C., Pérot, K., Fehr, T., Saavedra, L., Leppelmeier, G. W., and Fraisse, R.: Global ozone monitoring by occultation of stars: an overview of GOMOS measurements on ENVISAT, Atmos. Chem. Phys., 10, 12091–12148, doi:10.5194/acp-10-12091-2010, 2010. 3701

Boone, C. D., Nassar, R., Walker, K. A., Rochon, Y., McLeod, S. D., Rinsland, C. P., and Bernath, P. F.: Retrievals for the Atmospheric Chemistry Experiment Fourier Transform Spectrometer, Appl. Optics, 44, 7218–7231, 2005. 3703

Boone, C. D., Walker, K. A., and Bernath, P.F: Version 3 Retrievals for the Atmospheric Chemistry Experiment Fourier Transform Spectrometer (ACE-FTS), in: The Atmospheric Chemistry Experiment ACE at 10: A Solar Occultation Anthology, edited by: Bernath, P., Deepak Publishing, Hampton, Virginia, USA, 103–127, 2013. 3703

AMTD

8, 3697–3728, 2015

Relative drifts and biases between six ozone limb satellite measurements

N. Rahpoe et al.

Title Page
Abstract | Introduction
Conclusions | References
Tables | Figures
◂◂ | ▸▸
◂ | ▸
Back | Close
Full Screen / Esc
Printer-friendly Version
Interactive Discussion

Bourassa, A. E., Degenstein, D. A., Randel, W. J., Zawodny, J. M., Kyrölä, E., McLinden, C. A., Sioris, C. E., and Roth, C. Z.: Trends in stratospheric ozone derived from merged SAGE II and Odin-OSIRIS satellite observations, Atmos. Chem. Phys., 14, 6983–6994, doi:10.5194/acp-14-6983-2014, 2014. 3700

Bovensmann, H., Burrows, J. P., Buchwitz, M., Frerick, J., Noël, S., Rozanov, V. V., Chance, K. V., and Goede, A. P. H.: SCIAMACHY: mission objectives and measurement modes, J. Atmos. Sci., 56, 127–150, 1999. 3702

Bovensmann, H., Ahlers, B., Buchwitz, M., Frerick, J., Gottwald, M., Hoogeveen, R., Kaiser, J. W., Kleipool, Q., Krieg, E., Lichtenberg, G., Mager, R., Meyer, J., Noël, S., Schlesier, A., Sioris, C., Skupin, J., von Savigny, C., Wuttke, M. W., and Burrows, J. P.: SCIAMACHY in-flight instrument performance, Proceedings of the Envisat Calibration Review (SP-520), ESA Publications Division, 2002. 3702

Bovensmann, H., Aben, I., van Roozendael, M., Kühl, S., Gottwald, M., von Savigny, C., Buchwitz, M., Richter, A., Frankenberg, C., Stammes, P., de Graaf, M., Wittrock, F., Sinnhuber, M., Sinnhuber, B.-M., Schöhardt, A., Beirle, S., Gloudemans, A., Schrijver, H., Bracher, A., Rozanov, A., V., Weber, M., and Burrows, J. P.: SCIAMACHY's view of the changing earth's environment, in: SCIAMACHY – Exploring the Changing Earth's Atmosphere, edited by: Gottwald, M. and Bovensmann, H., Springer, Dordrecht, 175–216, 2011. 3702

Cortesi, U., Lambert, J. C., De Clercq, C., Bianchini, G., Blumenstock, T., Bracher, A., Castelli, E., Catoire, V., Chance, K. V., De Mazière, M., Demoulin, P., Godin-Beekmann, S., Jones, N., Jucks, K., Keim, C., Kerzenmacher, T., Kuellmann, H., Kuttippurath, J., Iarlori, M., Liu, G. Y., Liu, Y., McDermid, I. S., Meijer, Y. J., Mencaraglia, F., Mikuteit, S., Oelhaf, H., Piccolo, C., Pirre, M., Raspollini, P., Ravegnani, F., Reburn, W. J., Redaelli, G., Remedios, J. J., Sembhi, H., Smale, D., Steck, T., Taddei, A., Varotsos, C., Vigouroux, C., Waterfall, A., Wetzel, G., and Wood, S.: Geophysical validation of MIPAS-ENVISAT operational ozone data, Atmos. Chem. Phys., 7, 4807–4867, doi:10.5194/acp-7-4807-2007, 2007. 3702

Dupuy, E., Walker, K. A., Kar, J., Boone, C. D., McElroy, C. T., Bernath, P. F., Drummond, J. R., Skelton, R., McLeod, S. D., Hughes, R. C., Nowlan, C. R., Dufour, D. G., Zou, J., Nichitiu, F., Strong, K., Baron, P., Bevilacqua, R. M., Blumenstock, T., Bodeker, G. E., Borsdorff, T., Bourassa, A. E., Bovensmann, H., Boyd, I. S., Bracher, A., Brogniez, C., Burrows, J. P., Catoire, V., Ceccherini, S., Chabrillat, S., Christensen, T., Coffey, M. T., Cortesi, U., Davies, J., De Clercq, C., Degenstein, D. A., De Mazière, M., Demoulin, P., Dodion, J., Firanski, B., Fischer, H., Forbes, G., Froidevaux, L., Fussen, D., Gerard, P., Godin-Beekmann, S., Goutail,

AMTD

8, 3697–3728, 2015

Relative drifts and biases between six ozone limb satellite measurements

N. Rahpoe et al.

F., Granville, J., Griffith, D., Haley, C. S., Hannigan, J. W., Höpfner, M., Jin, J. J., Jones, A., Jones, N. B., Jucks, K., Kagawa, A., Kasai, Y., Kerzenmacher, T. E., Kleinböhl, A., Klekociuk, A. R., Kramer, I., Küllmann, H., Kuttippurath, J., Kyrölä, E., Lambert, J.-C., Livesey, N. J., Llewellyn, E. J., Lloyd, N. D., Mahieu, E., Manney, G. L., Marshall, B. T., McConnell, J. C., McCormick, M. P., McDermid, I. S., McHugh, M., McLinden, C. A., Mellqvist, J., Mizutani, K., Murayama, Y., Murtagh, D. P., Oelhaf, H., Parrish, A., Petelina, S. V., Piccolo, C., Pommereau, J.-P., Randall, C. E., Robert, C., Roth, C., Schneider, M., Senten, C., Steck, T., Strandberg, A., Strawbridge, K. B., Sussmann, R., Swart, D. P. J., Tarasick, D. W., Taylor, J. R., Tétard, C., Thomason, L. W., Thompson, A. M., Tully, M. B., Urban, J., Vanhellemont, F., Vigouroux, C., von Clarmann, T., von der Gathen, P., von Savigny, C., Waters, J. W., Witte, J. C., Wolff, M., and Zawodny, J. M.: Validation of ozone measurements from the Atmospheric Chemistry Experiment (ACE), Atmos. Chem. Phys., 9, 287–343, doi:10.5194/acp-9-287-2009, 2009. 3700, 3708

Eckert, E., von Clarmann, T., Kiefer, M., Stiller, G. P., Lossow, S., Glatthor, N., Degenstein, D. A., Froidevaux, L., Godin-Beekmann, S., Leblanc, T., McDermid, S., Pastel, M., Steinbrecht, W., Swart, D. P. J., Walker, K. A., and Bernath, P. F.: Drift-corrected trends and periodic variations in MIPAS IMK/IAA ozone measurements, Atmos. Chem. Phys., 14, 2571–2589, doi:10.5194/acp-14-2571-2014, 2014. 3700, 3709

Fischer, H., Birk, M., Blom, C., Carli, B., Carlotti, M., von Clarmann, T., Delbouille, L., Dudhia, A., Ehhalt, D., Endemann, M., Flaud, J. M., Gessner, R., Kleinert, A., Koopman, R., Langen, J., López-Puertas, M., Mosner, P., Nett, H., Oelhaf, H., Perron, G., Remedios, J., Ridolfi, M., Stiller, G., and Zander, R.: MIPAS: an instrument for atmospheric and climate research, Atmos. Chem. Phys., 8, 2151–2188, doi:10.5194/acp-8-2151-2008, 2008. 3701

Froidevaux, L., Anderson, J., Wang, R., and Fuller, R.: Long-term stratospheric data records from satellite records (GOZCARDS), NDACC Lidar WG Meeting, Table Mountain Facility, Wrightwood, CA, USA, 5 November 2013. 3700

Hassler, B., Petropavlovskikh, I., Staehelin, J., August, T., Bhartia, P. K., Clerbaux, C., Degenstein, D., Mazière, M. De, Dinelli, B. M., Dudhia, A., Dufour, G., Frith, S. M., Froidevaux, L., Godin-Beekmann, S., Granville, J., Harris, N. R. P., Hoppel, K., Hubert, D., Kasai, Y., Kurylo, M. J., Kyrölä, E., Lambert, J.-C., Levelt, P. F., McElroy, C. T., McPeters, R. D., Munro, R., Nakajima, H., Parrish, A., Raspollini, P., Remsberg, E. E., Rosenlof, K. H., Rozanov, A., Sano, T., Sasano, Y., Shiotani, M., Smit, H. G. J., Stiller, G., Tamminen, J., Tarasick, D. W., Urban, J., van der A, R. J., Veefkind, J. P., Vigouroux, C., von Clarmann, T., von Savigny, C., Walker, K. A., Weber, M., Wild, J., and Zawodny, J. M.: Past changes in the vertical distribution of ozone – Part 1: Measurement techniques, uncertainties and availability, Atmos. Meas. Tech., 7, 1395–1427, doi:10.5194/amt-7-1395-2014, 2014. 3699, 3701

Kyrölä, E., Tamminen, J., Leppelmeier, G. W., Sofieva, V., Hassinen, S., Bertaux, J. L., Hauchecorne, A., Dalaudier, F., Cot, C., Korablev, O., Fanton d'Andon, O., Barrot, G., Mangin, A., Théodore, B., Guirlet, M., Etanchaud, F., Snoeij, P., Koopman, R., Saavedra, L., Fraisse, R., Fussen, D., and Vanhellemont, F.: GOMOS on Envisat, an overview, Adv. Space Res., 33, 1020–1028, 2004. 3701

Kyrölä, E., Tamminen, J., Sofieva, V., Bertaux, J. L., Hauchecorne, A., Dalaudier, F., Fussen, D., Vanhellemont, F., Fanton d'Andon, O., Barrot, G., Guirlet, M., Mangin, A., Blanot, L., Fehr, T., Saavedra de Miguel, L., and Fraisse, R.: Retrieval of atmospheric parameters from GOMOS data, Atmos. Chem. Phys., 10, 11881–11903, doi:10.5194/acp-10-11881-2010, 2010. 3701

Kyrölä, E., Laine, M., Sofieva, V., Tamminen, J., Päivärinta, S.-M., Tukiainen, S., Zawodny, J., and Thomason, L.: Combined SAGE II–GOMOS ozone profile data set for 1984–2011 and trend analysis of the vertical distribution of ozone, Atmos. Chem. Phys., 13, 10645–10658, doi:10.5194/acp-13-10645-2013, 2013. 3700

Laeng, A., Grabowski, U., von Clarmann, T., Stiller, G., Glatthor, N., Höpfner, M., Kellmann, S., Kiefer, M., Linden, A., Lossow, S., Sofieva, V., Petropavlovskikh, I., Hubert, D., Bathgate, T., Bernath, P., Boone, C. D., Clerbaux, C., Coheur, P., Damadeo, R., Degenstein, D., Frith, S., Froidevaux, L., Gille, J., Hoppel, K., McHugh, M., Kasai, Y., Lumpe, J., Rahpoe, N., Toon, G., Sano, T., Suzuki, M., Tamminen, J., Urban, J., Walker, K., Weber, M., and Zawodny, J.: Validation of MIPAS IMK/IAA V5R_O3_224 ozone profiles, Atmos. Meas. Tech., 7, 3971–3987, doi:10.5194/amt-7-3971-2014, 2014. 3700, 3702

Llewellyn, E. J., Lloyd, N. D., Degenstein, D. A., Gattinger, R. L., Petelina, S. V., Bourassa, A. E., Wiensz, J. T., Ivanov, E. V., McDade, I. C., Solheim, B. H., McConnell, J. C., Haley, C. S., von Savigny, C., Sioris, C. E., McLinden, C. A., Griffioen, E., Kaminski, J., Evans, W. F. J., Puckrin, E., Strong, K., Wehrle, V., Hum, R. H., Kendall, D. J. W., Matsushita, J., Murtagh, D. P., Brohede, S., Stegman, J., Witt, G., Barnes, G., Payne, W. F., Piché, L., Smith, K., Warshaw, G., Deslauniers, D.-L., Marchand, P., Richardson, E. H., King, R. A., Wevers, I., McCreath, W., Kyrölä, E., Oikarinen, L., Leppelmeier, G. W., Auvinen, H., Mégie, G., Hauchecorne, A., Lefèvre, F., de La Nöe, J., Ricaud, P., Frisk, U., Sjoberg, F., von Schéele, F., and Nordh, L.: The OSIRIS Instrument on the Odin Spacecraft, Can. J. Phys., 82, 411–422, 2004. 3702

Mieruch, S., Weber, M., von Savigny, C., Rozanov, A., Bovensmann, H., Burrows, J. P., Bernath, P. F., Boone, C. D., Froidevaux, L., Gordley, L. L., Mlynczak, M. G., Russell III, J. M., Thomason, L. W., Walker, K. A., and Zawodny, J. M.: Global and long-term comparison of SCIAMACHY limb ozone profiles with correlative satellite data (2002–2008), Atmos. Meas. Tech., 5, 771–788, doi:10.5194/amt-5-771-2012, 2012. 3700, 3702

Murtagh, D., Frisk, U., Merino, M., Ridal, F., Jonsson, A., Stegman, J., Witt, G., Eriksson, P., Jiménez, C., Megie, G., de la Nöe, J., Ricaud, P., Baron, P., Hauchcorne, A., Llewellyn, E. J., Degenstein, D. A., Gattinger, R. L., Lloyd, N. D. Evans, W. F. J., McDade, I. C., Haley, C. S. Sioris, C., von Savigny, C., Solheim, B. H., McConnell, J. C., Strong, K., Richardson, E. H., Leppelmeier, G. W., Kyrölä, E., Auvinen, H., and Oikarinen, L.: An overview of the Odin atmospheric mission, Can. J. Phys., 80, 309–319, 2002. 3702

Rahpoe, N., von Savigny, C., Weber, M., Rozanov, A.V., Bovensmann, H., and Burrows, J. P.: Error budget analysis of SCIAMACHY limb ozone profile retrievals using the SCIATRAN model, Atmos. Meas. Tech., 6, 2825–2837, doi:10.5194/amt-6-2825-2013, 2013. 3702

Rozanov, A., Rozanov, V. V., and Burrows, J. P.: A numerical radiative transfer model for a spherical planetary atmosphere: combined differential-integral approach involving the Picard iterative approximation, J. Quant. Spectrosc. Ra., 69, 491–512, 2001. 3702

Sonkaew, T., Rozanov, V. V., von Savigny, C., Rozanov, A., Bovensmann, H., and Burrows, J. P.: Cloud sensitivity studies for stratospheric and lower mesospheric ozone profile retrievals from measurements of limb-scattered solar radiation, Atmos. Meas. Tech., 2, 653–678, doi:10.5194/amt-2-653-2009, 2009. 3702

Sofieva, V. F., Rahpoe, N., Tamminen, J., Kyrölä, E., Kalakoski, N., Weber, M., Rozanov, A., von Savigny, C., Laeng, A., von Clarmann, T., Stiller, G., Lossow, S., Degenstein, D., Bourassa, A., Adams, C., Roth, C., Lloyd, N., Bernath, P., Hargreaves, R. J., Urban, J., Murtagh, D., Hauchecorne, A., Dalaudier, F., van Roozendael, M., Kalb, N., and Zehner, C.: Harmonized dataset of ozone profiles from satellite limb and occultation measurements, Earth Syst. Sci. Data, 5, 349–363, doi:10.5194/essd-5-349-2013, 2013. 3701

Steck, T., von Clarmann, T., Fischer, H., Funke, B., Glatthor, N., Grabowski, U., Höpfner, M., Kellmann, S., Kiefer, M., Linden, A., Milz, M., Stiller, G. P., Wang, D. Y., Allaart, M., Blumenstock, Th., von der Gathen, P., Hansen, G., Hase, F., Hochschild, G., Kopp, G., Kyrö, E., Oelhaf, H., Raffalski, U., Redondas Marrero, A., Remsberg, E., Russell III, J., Stebel, K., Steinbrecht, W., Wetzel, G., Yela, M., and Zhang, G.: Bias determination and precision validation of ozone profiles from MIPAS-Envisat retrieved with the IMK-IAA processor, Atmos. Chem. Phys., 7, 3639–3662, doi:10.5194/acp-7-3639-2007, 2007. 3700

Tamminen, J., Kyrölä, E., Sofieva, V. F., Laine, M., Bertaux, J.-L., Hauchecorne, A., Dalaudier, F., Fussen, D., Vanhellemont, F., Fanton-d'Andon, O., Barrot, G., Mangin, A., Guirlet, M., Blanot, L., Fehr, T., Saavedra de Miguel, L., and Fraisse, R.: GOMOS data characterisation and error estimation, Atmos. Chem. Phys., 10, 9505–9519, doi:10.5194/acp-10-9505-2010, 2010. 3701

Tegtmeier, S., Hegglin, M. I., Anderson, J., Bourassa, A., Brohede, S., Degenstein, D., Froidevaux, L., Fuller, R., Funke, B., Gille, J., Jones, A., Kasai, Y., Krüger, K., Kyrölä, E., Lingenfelser, Lumpe, J., Nardi, B., Neu, J., Pendlebury, D., Remsberg, E., Rozanov, A., Smith, L., Toohey, M., Urban, J., von Clarmann, T., Walker, K. A., and Wang, H. J.: The SPARC Data Initiative: a comparison of ozone climatologies from international satellite limb sounders, J. Geophys. Res., 18, 12229–12247, doi:10.1002/2013JD019877, 2013. 3700

Urban, J., Lautié, N., Le Flochmoë, E., Jiménez, C, Eriksson, P., de La Noë, J, Dupuy, E., Ekström, M., El Amraoui, L., Frisk, U, Murtagh, D., Olberg, M., and Ricaud, P.: Odin/SMR observations of stratospheric trace gases: level 2 processing of ClO, N_2O,O_3, HNO_3, J. Geophys. Res., 110, D14307, doi:10.1029/2004JD005741, 2005. 3703

Table 1. Number of total collocations (90° S–90° N) for pairwise combinations.

Pairs	SCIA	GOMOS	OSIRIS	MIPAS	ACE	SMR
SCIAMACHY	–	155 825	429 500	605 174	16 340	129 832
GOMOS	–	–	276 712	65 284	9737	23 043
OSIRIS	–	–	–	900 552	8471	248 703
MIPAS	–	–	-	–	8726	140 876
ACE	–	–	–	–	–	11 356

AMTD
8, 3697–3728, 2015

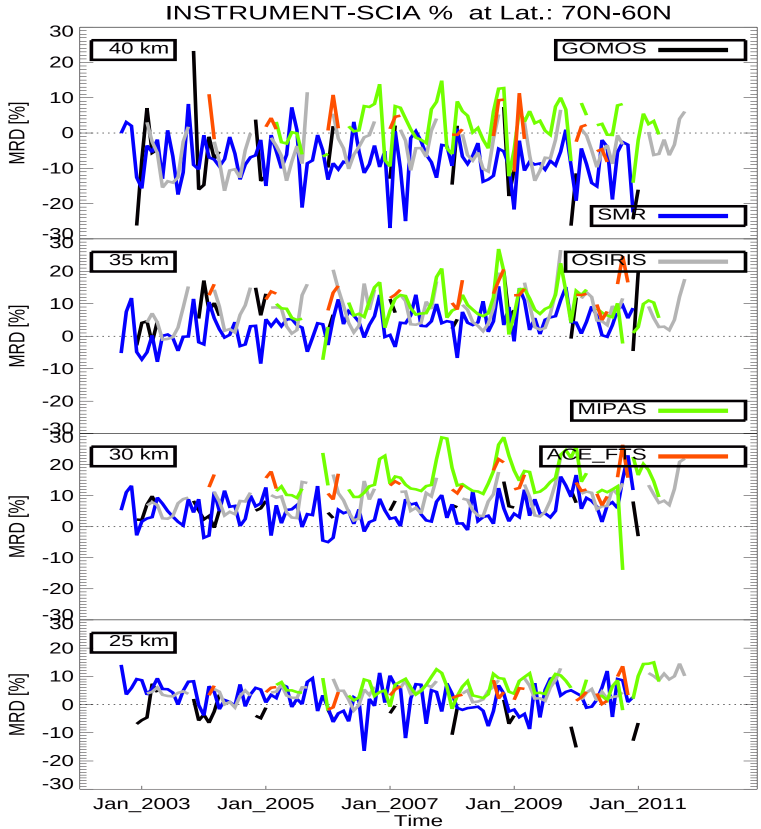

Figure 1. Mean relative difference $\Delta(z)$ time series between all instruments (comparison sensor) and SCIAMACHY (reference sensor) in the latitude band 70–60° N.

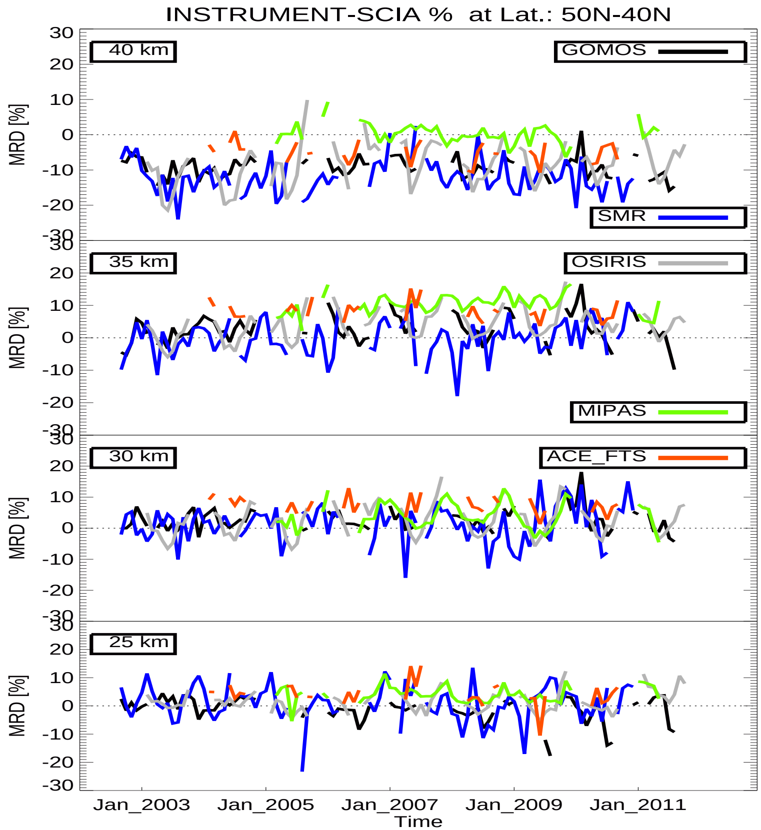

Figure 2. Same as Fig. 1, but for northern middle latitudes (50–40° N).

AMTD
8, 3697–3728, 2015

Relative drifts and biases between six ozone limb satellite measurements

N. Rahpoe et al.

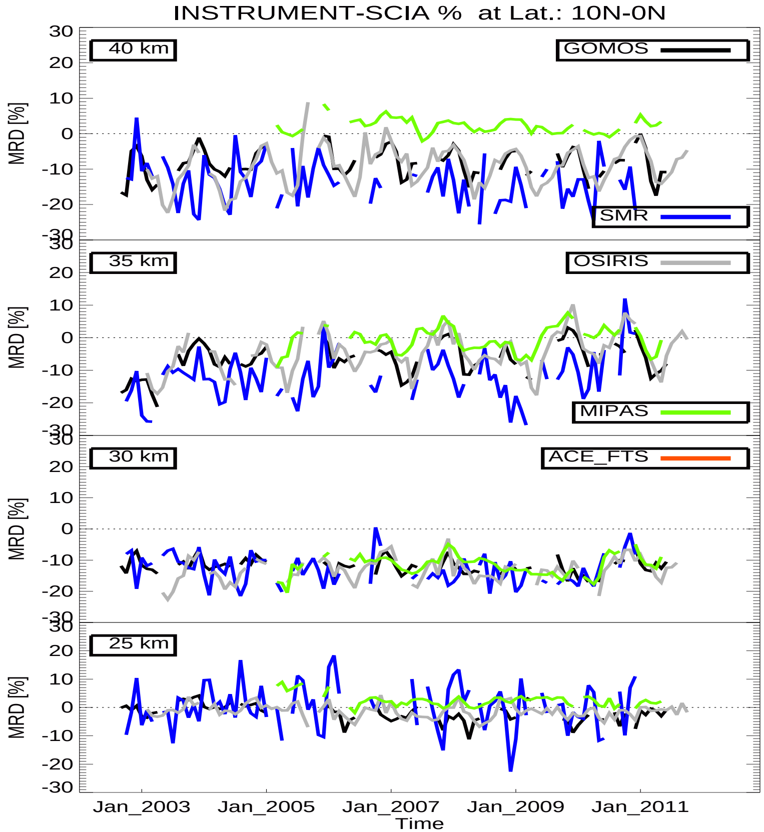

Figure 3. Same as Fig. 2, but for tropical latitude (10–0° N).

AMTD
8, 3697–3728, 2015

Relative drifts and biases between six ozone limb satellite measurements

N. Rahpoe et al.

Title Page
Abstract Introduction
Conclusions References
Tables Figures
◀| |▶
◀ ▶
Back Close
Full Screen / Esc
Printer-friendly Version
Interactive Discussion

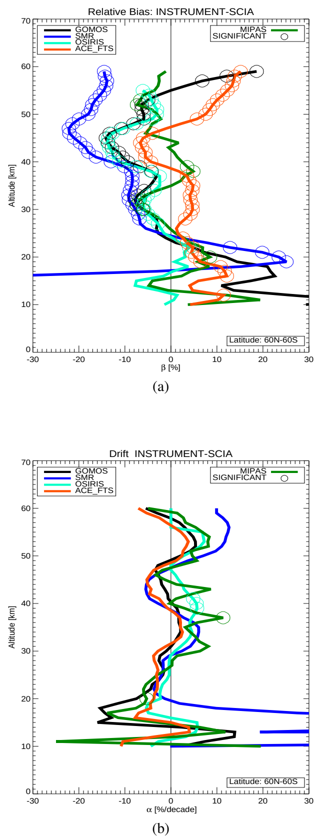

Figure 4. Near global "pairwise relative bias" β (top) and relative drift α (bottom) profiles of all sensors with respect to SCIAMACHY. Different colours correspond to comparison instruments. Open circles indicate statistically significant values at confidence interval CI = 95 %, i.e., $(\alpha,\beta) > 2\sigma_{(\alpha,\beta)}$.

AMTD
8, 3697–3728, 2015

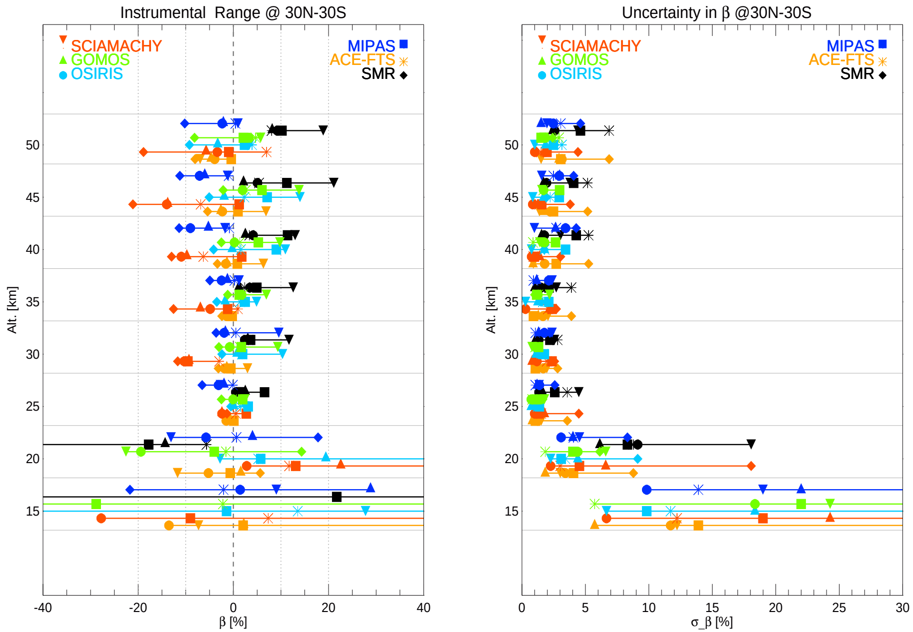

Figure 5. (a) "Pairwise relative bias" (β) range for all sensors as a function of altitude. Reference sensors are indicated by colour and individual comparison sensors by corresponding symbols. **(b)** Corresponding uncertainties σ_β.

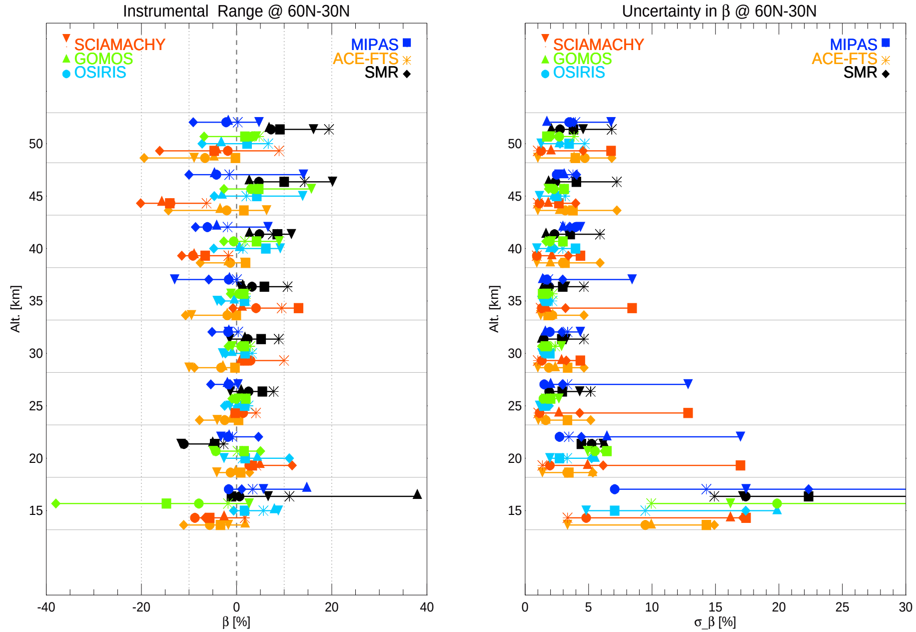

Figure 6. Same as Fig. 5 buf for the northern middle latitudes (60–30° N).

AMTD
8, 3697–3728, 2015

Relative drifts and biases between six ozone limb satellite measurements

N. Rahpoe et al.

Title Page
Abstract Introduction
Conclusions References
Tables Figures
◀◀ ▶▶
◀ ▶
Back Close
Full Screen / Esc
Printer-friendly Version
Interactive Discussion

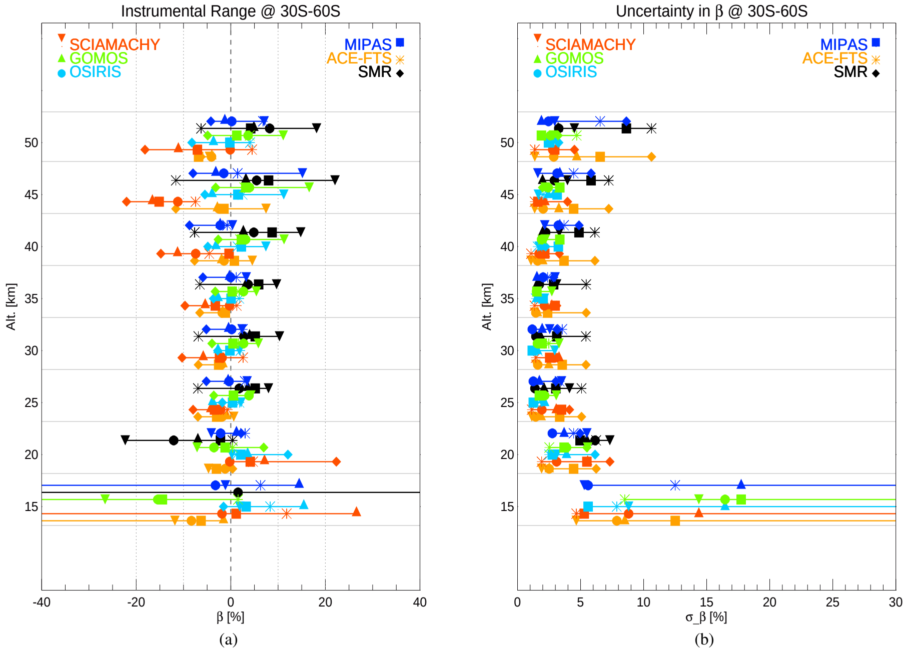

Figure 7. Same as Fig. 5 buf for the southern middle latitudes (30–60° S).

AMTD
8, 3697–3728, 2015

Relative drifts and biases between six ozone limb satellite measurements

N. Rahpoe et al.

Title Page
Abstract Introduction
Conclusions References
Tables Figures
◄ ►
Back Close
Full Screen / Esc
Printer-friendly Version
Interactive Discussion

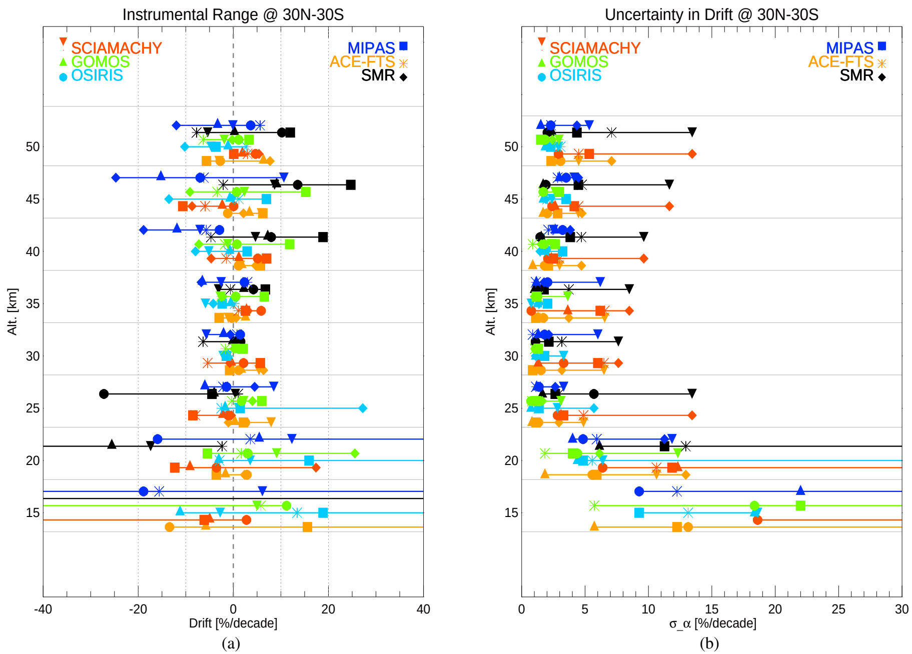

Figure 8. (a) Relative drift (α) range for all sensors as a function of altitude. Reference sensors are indicated by colour and individual comparison sensors by corresponding symbols. **(b)** Corresponding uncertainty σ_α.

AMTD

8, 3697–3728, 2015

Relative drifts and biases between six ozone limb satellite measurements

N. Rahpoe et al.

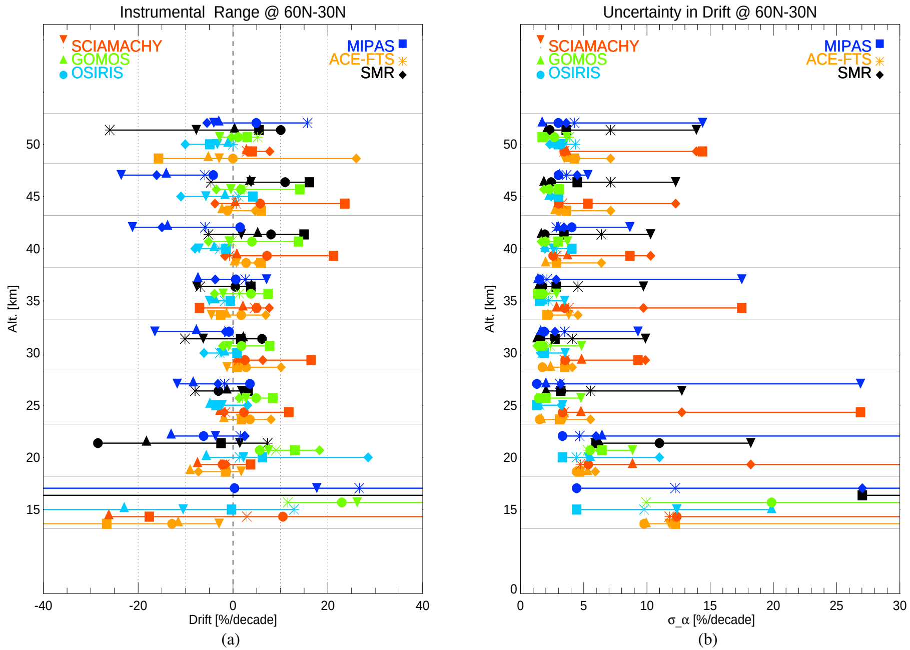

Figure 9. Same as Fig. 8 buf for the northern middle latitudes (60–30° N).

AMTD
8, 3697–3728, 2015

Relative drifts and biases between six ozone limb satellite measurements

N. Rahpoe et al.

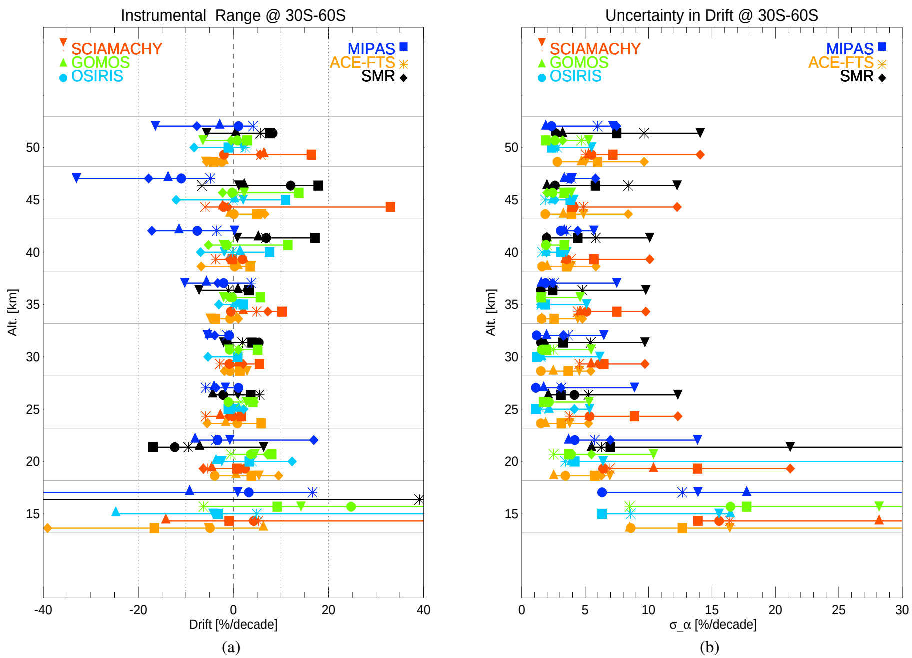

Figure 10. Same as Fig. 8 buf for the southern middle latitudes (30–60° S).

AMTD
8, 3697–3728, 2015

Relative drifts and biases between six ozone limb satellite measurements

N. Rahpoe et al.

Title Page
Abstract Introduction
Conclusions References
Tables Figures
Back Close
Full Screen / Esc
Printer-friendly Version
Interactive Discussion